JBC RESEARCH ARTICLE

ADAR1- and ADAR2-mediated regulation of maturation and targeting of miR-376b to modulate GABA neurotransmitter catabolism

Received for publication, October 19, 2021, and in revised form, January 31, 2022 Published, Papers in Press, February 3, 2022,
https://doi.org/10.1016/j.jbc.2022.101682

Albin Widmark[1,*], Eduardo A. Sagredo[1,2], Victor Karlström[1], Mikaela Behm[1], Inna Biryukova[2], Marc R. Friedländer[2], Chammiran Daniel[1], and Marie Öhman[1]

From the [1]Department of Molecular Biosciences, and [2]Science for Life Laboratory, Department of Molecular Biosciences, The Wenner-Gren Institute, Stockholm University, Stockholm, Sweden

Edited by Karin Musier-Forsyth

miRNAs are short noncoding RNA molecules that regulate gene expression by inhibiting translation or inducing degradation of target mRNAs. miRNAs are often expressed as polycistronic transcripts, so-called miRNA clusters, containing several miRNA precursors. The largest mammalian miRNA cluster, the miR-379–410 cluster, is expressed primarily during embryonic development and in the adult brain; however, downstream regulation of this cluster is not well understood. Here, we investigated adenosine deamination to inosine (RNA editing) in the miR-379–410 cluster by adenosine deaminase acting on RNA (ADAR) enzymes as a possible mechanism modulating the expression and activity of these miRNAs in a brain-specific manner. We show that the levels of editing in the majority of mature miRNAs are lower than the editing levels of the corresponding site in primary miRNA precursors. However, for one miRNA, miR-376b-3p, editing was significantly higher in the mature form than in the primary precursor. We found miR-376b-3p maturation is negatively regulated by ADAR2 in an editing activity–independent manner, whereas ADAR1-mediated and ADAR2-mediated editing were observed to be competitive. In addition, the edited miR-376b-3p targets a different set of mRNAs than unedited miR-376b-3p, including 4-aminobutyrate aminotransferase, encoding the enzyme responsible for the catabolism of the neurotransmitter gamma aminobutyric acid (GABA). Expression of edited miR-376b-3p led to increased intracellular GABA levels as well as increased cell surface presentation of GABA type A receptors. Our results indicate that both editing and editing-independent effects modulate the expression of miR-376b-3p, with the potential to regulate GABAergic signaling in the brain.

miRNAs are short noncoding RNA that act as post-transcriptional regulators of gene expression by inhibiting translation and/or inducing degradation of target mRNAs (1). miRNAs are transcribed as primary-miRNAs (pri-miRNAs), which are hairpin structures of dsRNA structure. pri-miRNAs are recognized by a complex consisting of the RNA-binding protein DiGeorge syndrome critical region 8 and the endonuclease Drosha, which cleaves the dsRNA structure, releasing a ∼70 nucleotide (nt) precursor miRNA (pre-miRNA) (2). The pre-miRNA is then exported to the cytoplasm, where it is recognized by Dicer that cleaves the hairpin structure again, releasing a duplexed pair of mature miRNAs (3). One strand of the duplex is then incorporated into the RNA-induced silencing complex (RISC), whereupon it serves to guide the complex to mRNAs containing complementary sequences. The region of nucleotides 2 to 8 of the miRNA is critical for targeting and is termed the seed region (4). miRNA genes are often found clustered in the genome and are expressed as a single polycistronic transcript, which contains several pri-miRNA hairpins (5, 6). This enables coordinated transcriptional regulation of miRNAs involved in the same biological function or regulatory network (7). Post-transcriptional regulation of miRNA expression, involving mechanisms affecting steps in miRNA biogenesis and/or miRNA turnover, enables modulation of levels of individual miRNAs within a cluster (8).

The largest miRNA cluster in mammals is the miR-379–410 cluster, which contains as many as 39 pri-miRNA genes in a ∼40 kB region (9, 10). This cluster is widely expressed in the developing mouse, whereas expression becomes mostly restricted to the brain in the adult mouse (11). Mice lacking the miR-379–410 cluster display phenotypes in agreement with a dual function of the cluster members in development and in the adult brain, as the miR-379–410 cluster–deficient mice display partially penetrant neonatal lethality because of metabolic defects as well as enhanced anxiety-related and hypersocial behavior of the adult mice (10–12). These behavioral alterations were coupled to an increased excitatory synaptic transmission and spine density of hippocampal neuronal cultures (12). In the hippocampal transcriptome, deletion of the miR-379–410 cluster led to increased expression of glutamate receptor components and decreased expression of genes related to gamma aminobutyric acid (GABA)ergic signaling (12). Components of the glutamatergic signaling pathway were also found to be upregulated following deletion

* For correspondence: Albin Widmark, albin.widmark@su.se.
Present address for Mikaela Behm: German Cancer Research Center - Deutsches Krebsforschungszentrum (DKFZ), Im Neuenheimer Feld 280, Heidelberg 69120, Germany.

of the miR-379–410 cluster in induced neuronal cell cultures (13). Individual members of the miRNA cluster have also been studied in a neuronal context, with miRNAs suggested to regulate processes, such as neurogenesis, neuronal migration, and synaptic plasticity (reviewed in Ref. (14)). Expression patterns of individual members of the cluster in different tissues and different developmental stages indicate that post-transcriptional mechanisms modulate the expression of individual miRNAs from the cluster (13).

Several members of the miR-379–410 cluster have been found to be subjected to adenosine-to-inosine (A-to-I) RNA editing (15, 16). This biological process consists of the enzymatic deamination of specific adenosines within dsRNA structures catalyzed by the adenosine deaminase acting on RNA (ADAR) family of enzymes. The resulting inosine has base-pairing characteristics similar to those of guanosine, which means that editing of a miRNA generates a form that has a different set of target mRNAs (15, 17, 18). Editing of pri-miRNA can also influence miRNA biogenesis, often preventing pri-miRNA processing (19) though cases where RNA editing makes miRNA processing more efficient have also been reported (20). In addition, the ADAR enzymes bind dsRNA structures such as those found in pri-miRNA hairpins and can thereby influence miRNA biogenesis in an editing-independent way (21). The two ADAR enzymes, ADAR1 and ADAR2, have different editing site specificities (22) and can have different effects on miRNA biogenesis (21). In addition, ADAR1 is expressed as two different isoforms, a shorter p110 isoform localized in the nucleus and a longer interferon-induced p150 isoform that shuttles between the nucleus and the cytoplasm (23, 24). Variable expression of the ADAR enzymes in different tissues and different developmental stages may contribute to differential miRNA regulation (25, 26).

In mammals, ADAR expression and miRNA editing are highly enriched in the brain, and editing of neural miRNAs has been found to retarget miRNAs to mRNAs involved in learning, memory, and cognition (26). miRNA editing in the mammalian brain is also developmentally regulated, with miRNA editing increasing during brain development (27). The extensive editing of the miR-379–410 cluster in the adult mouse brain, which is absent in the embryonically expressed miRNA cluster (28), is likely to be a mechanism for modulating miRNA expression and targeting in a tissue-specific manner. Here, we show that expression and editing of miR-376b-3p is developmentally modulated by ADAR1 and ADAR2, with increased levels of edited miR-376b-3p in later stages of mouse brain development. Furthermore, edited miR-376b-3p regulates the mRNA levels of genes involved in neuronal function. These genes include 4-aminobutyrate aminotransferase (*Abat*), suggesting a connection between miR-376b-3p editing and regulation of GABAergic signaling in the brain.

Results

Editing of the miR-379–410 cluster

The miR-379–410 cluster contains eight miRNAs that are subjected to A-to-I RNA editing (15, 19, 27). To analyze if RNA editing affects the maturation of these miRNAs in the developing brain, we first compared the editing levels between the primary transcript and corresponding site in the mature miRNA in juvenile mouse brain (Fig. 1*A*). Seven of the eight sites analyzed showed different editing levels between the two stages of miRNA maturation. For these seven sites, six sites had significantly lower editing in the mature miRNA

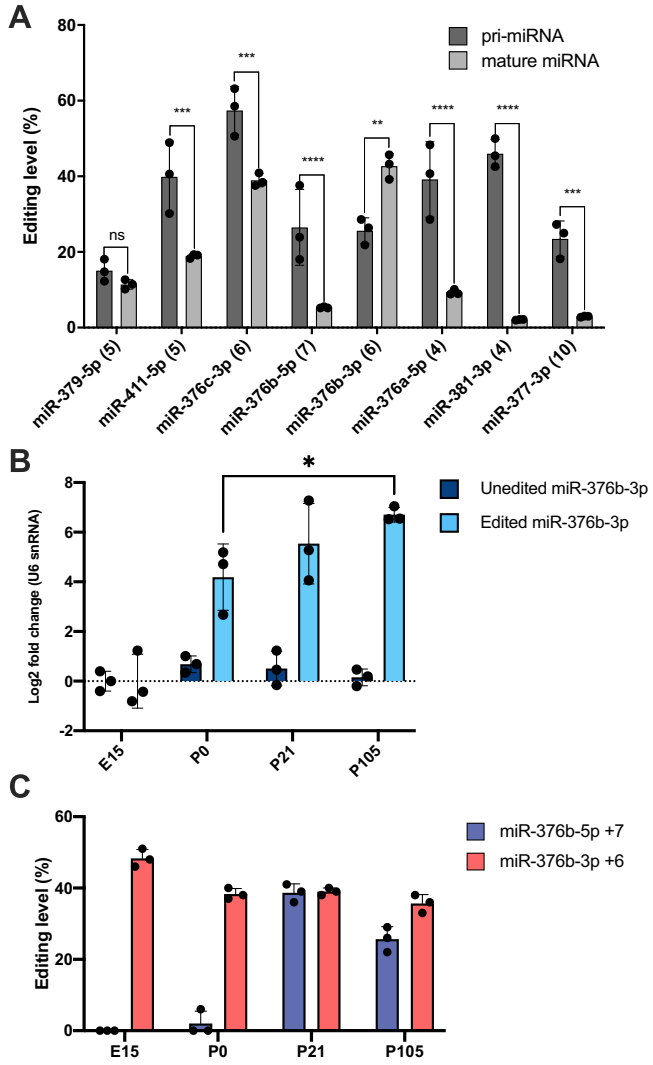

Figure 1. Expression and editing of miR-376b-3p during mouse brain development. *A*, comparing the editing levels of pri-miRNAs of the miR-379–410 cluster to the corresponding sites in the mature miRNAs. The sequenced RNA was purified from 6- to 8-week-old mouse brains, in biological triplicate. Pri-miRNAs were sequenced by performing reverse transcription with gene-specific primers for the seven pri-miRNAs, followed by sequencing of cDNA. Mature miRNA was sequenced by isolating small RNAs and performing RNA-Seq. *B*, miRNA-specific LNA-based qPCR was performed on mouse brains at four different developmental stages: embryonic day 15 (E15), at birth (P0), 3 weeks after birth (P21), and adult (P105) (n = 3). The primers used were able to distinguish between edited and unedited miR-376b-3p. Expression levels were calculated as ΔΔCt, with normalization to expression of U6 snRNA and calculated as log2 fold change compared with E15. *C*, editing of pri-miR-376b during mouse brain development. RNA from the samples mentioned previously was used for an RT–PCR with primers amplifying pri-miR-376b. The PCR products were analyzed by Sanger sequencing to determine editing levels of the two main sites of the pri-miRNA, by dividing the height of the G-peak in the chromatogram with the sum of the A-peak and G-peak. cDNA, complementary DNA; LNA, locked nucleic acid; pri-miRNA, primary-miRNA; qPCR, quantitative PCR.

compared with the pri-miRNA. For instance, the editing site in miR-381-3p, where the pri-miRNA was edited to 46%, whereas the editing of the corresponding site in the mature form was only 2%. This suggests that RNA editing of the miR-379–410 cluster generally inhibits miRNA maturation. However, unlike the other miRNAs of the cluster, miR-376b-3p editing was significantly higher in the mature miRNA (43%) compared with the pri-miRNA (26%), being one of the most highly edited mature miRNAs. In order to investigate this observation and how ADAR enzymes can affect miRNAs of the cluster, we selected this miRNA for further study.

Editing of miR-376b during brain development

Since A-to-I RNA editing of miRNA has been found to be developmentally regulated (27), we performed a quantitative PCR (qPCR) assay of miR-376b-3p in different stages of brain development in order to investigate how miR-376b editing is connected to expression levels during brain development. We performed RT–qPCR using locked nucleic acid (LNA) primers able to distinguish between unedited and edited miR-376b-3p (as shown in Fig. S1). We analyzed the expression of the two forms of miR-376b-3p in mouse brains at four different developmental stages: embryonic day 15 (E15), birth (P0), 3 weeks after birth (P21), and adult (P105) (Fig. 1*B*). The levels of the edited miR-376b-3p isoform increased significantly during brain development, whereas the unedited isoform remained constant, in agreement with previously reported increased editing of miR-376b-3p (27).

Next, we investigated if the abundance of unedited and edited mature miR-376b isoforms correlated with the editing activity in the primary transcript. The pri-miR-376b contains two edited sites in the mature miRNAs, the +7 site in the 5p arm edited by ADAR2 and the +6 site in the 3p arm that is edited by ADAR1 (15, 20, 28). To measure editing at these sites during brain development, we performed Sanger sequencing of RT–PCR products of the pri-miR-376b transcript for the four developmental time points (Fig. 1*C*). Surprisingly, editing of the 3p +6 site remained fairly constant at 40 to 50%, and we did not see any increase between stages E15 and P0, as would be expected given the levels of edited miR-376b-3p. Editing of the 5p +7 site was absent at E15 and 2% at P0, after which it increased to 39% at P21, matching the previously reported developmental increase in ADAR2 activity (29). The observation that levels of edited miR-376b-3p increase without a concurrent increase in pri-miRNA editing at the corresponding site raises the possibility that editing regulates pri-miR-376b maturation.

ADAR2 prevents ADAR1-mediated editing of pri-miR-376b

To investigate the mechanism of pri-miR-376b editing and the roles of ADAR1 and ADAR2, we generated a pri-miR-376b expression vector, containing the pri-miRNA hairpin and ~200 nt of flanking sequence. The pri-miRNA expression vector was cotransfected in human embryonic kidney-293 (HEK-293) cells with expression vectors for the ADAR enzymes, either wildtype or containing a glutamate-to-alanine (E/A) change to inactivate the enzymes (Fig. S2) (30, 31). Sanger sequencing was performed on RT–PCR products to determine editing activity at the two sites of pri-miR-376b. As previously reported (19, 20, 28), we observed a clear enzymatic specificity for the two sites, with ADAR1 p110 editing the 3p +6 site at about 40% (Fig. 2*A*) and ADAR2 editing the 5p +7 site at a similar level (Fig. 2*B*). ADAR1 was able to edit the site on the 5p +7 site to 4%, whereas ADAR2 was unable to induce editing of the 3p +6 site. In fact, ADAR2 overexpression resulted in a trend of lower editing level at the 3p +6 site than those observed as a result of the endogenous editing in HEK-293 cells (Ctrl). This result could indicate that ADAR2 is able to block ADAR1-mediated editing of the 3p +6 site. Indeed, simultaneous overexpression of both ADAR1 p110 and ADAR2 completely prevented the editing mediated by ADAR1 p110 at the 3p +6 site. ADAR2 was however unable to significantly inhibit ADAR1 p150-mediated editing. Cotransfecting ADAR1 and ADAR2 simultaneously did not affect ADAR2-mediated editing of the 5p +7 site, indicating that ADAR1 p110 and p150 are both unable to prevent ADAR2-mediated editing. Enzymatically inactive ADAR2 (glutamate-to-alanine change) had the same inhibitory effect on ADAR1-mediated editing of the 3p +6 site, showing that the effect is editing independent. These results confirm the specificity of the two ADAR enzymes for each of the two editing sites of pri-miR-376b and suggest that ADAR2 can prevent ADAR1-mediated editing of pri-miR-376b in an editing-independent manner (Fig. 2*C*).

ADAR2 decreases abundance of mature miR-376b-5p and 3p in an editing-independent manner

Given the enrichment of ADAR1-mediated editing in contrast to the depletion of ADAR2-mediated editing in the mature forms of miR-376b in mouse brain, we next investigated the contribution of the different ADAR enzymes to miR-376b maturation. To measure the activity of miR-376b-3p, we inserted three miR-376b-3p binding sites in tandem in the 3′ UTR of firefly luciferase in a dual luciferase reporter construct. This reporter system was cotransfected with the previously described pri-miR-376b expression vector and the ADAR expression vectors (Fig. 3*A*). Cotransfecting with ADAR1 p110 did not affect the luciferase silencing levels, whereas ADAR1 p150 led to a slightly decreased luciferase signal. ADAR2 cotransfection resulted in derepression in an editing-independent manner, possibly reflecting that ADAR2 has an inhibitory effect on miR-376b-3p maturation. To determine whether the ADAR enzymes also affect the maturation of the opposite strand miRNA, we performed a similar experiment with a dual luciferase reporter for miR-376b-5p (Fig. 3*B*). The different forms of ADAR1 were not found to affect miR-376b-5p activity. However, as for the 3p miRNA, ADAR2 had an editing-independent inhibitory effect.

In order to verify that the ADAR-mediated effects are editing independent, we generated miRNA expression vectors in which the editing sites in the 5p or the 3p miRNAs were replaced by a guanosine (pre-editing), mimicking the presence

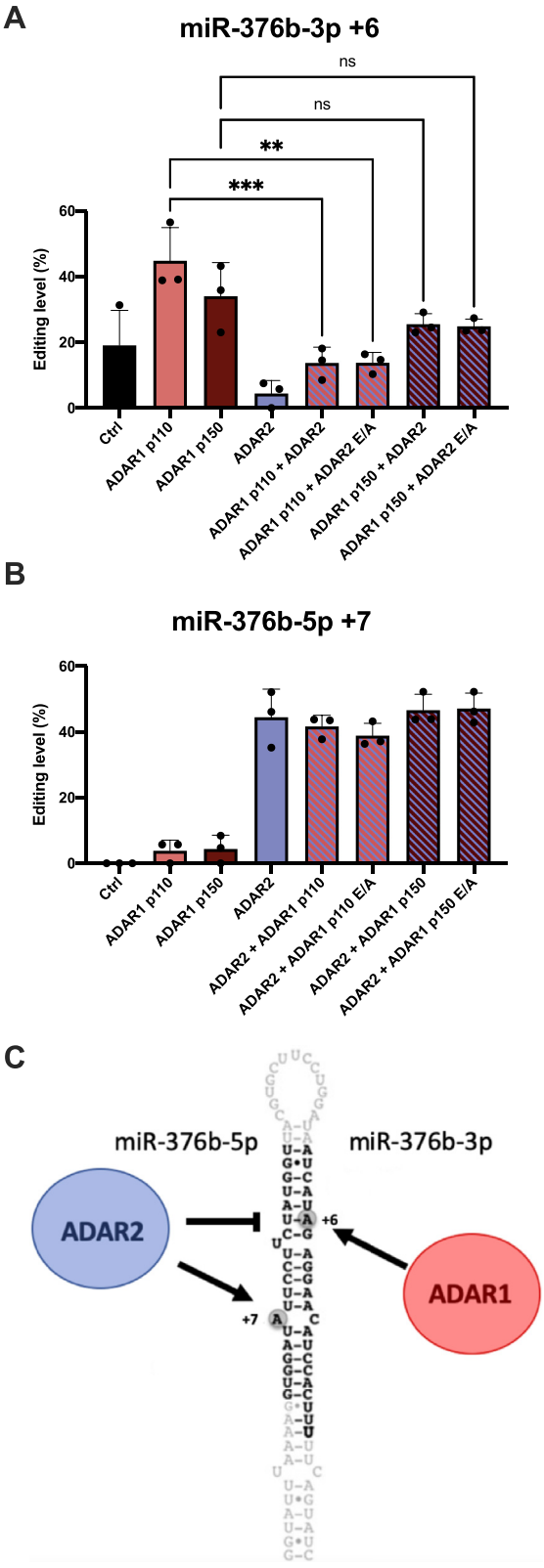

Figure 2. The mechanism of pri-miR-376b editing. *A* and *B*, an miR-376b expression vector was cotransfected with ADAR enzymes whereupon RT–PCR and Sanger sequencing were used to determine editing levels at the two editing sites: 3p +6 (*A*) and 5p +7 (*B*). ADAR enzymes were either wildtype or enzymatically inactivated by a glutamate-to-alanine (E/A) substitution. The editing level was calculated by dividing the height of the G-peak in the Sanger sequencing chromatogram with the sum of the A-peak and G-peak. *C*, a schematic illustration of the miR-376b hairpin, the two editing sites, and the enzymes influencing their editing. ADAR, adenosine deaminase acting on RNA.

of inosine. In order to preserve the targeting of the luciferase reporter, the complementary bases in the reporter were exchanged for cytosine. Here, we could verify that pre-editing of either the 5p or the 3p miRNA did not affect silencing of the miR-376b-3p luciferase reporter (Fig. 3*C*). Similarly, pre-editing of the 5p +7 site did not affect silencing of the miR-376b-5p reporter (Fig. 3*D*). However, 3p +6 pre-editing led to a significant decrease of miR-376b-5p reporter silencing, matching the inhibitory effect on miR-376b-5p expression seen when cotransfected with wildtype ADAR1 p110. These results verify the editing-independent nature of the previously observed effects of ADAR1 and ADAR2 on miR-376b-3p while suggesting that maturation of miR-376b-5p is inhibited by editing the 3p +6 site.

In the aforementioned luciferase assay, a decreased silencing activity could also be the result of an editing-induced mismatch in the miRNA–mRNA complementarity. To exclude this possibility and verify the results of the dual luciferase assay, we performed miRNA-specific qPCR of miR-376b-3p following cotransfection of miRNA expression vector and ADAR enzymes (Fig. 3, *E* and *F*). Levels of unedited miR-376b-3p did not change following cotransfection with ADAR1 p110, whereas ADAR1 p150 led to an increase (Fig. 3*E*). Overexpression of ADAR1 p110 resulted in a ∼10-fold increase of edited miR-376b-3p, likely corresponding to a 10-fold increase in miRNA editing, whereas p150 did not change levels of edited miRNA (Fig. 3*F*). In agreement with results from the dual luciferase assay shown in Figure 3, *A* and *B*, ADAR2 reduced miRNA levels, for both unedited and edited forms of the miRNA. In summary, these results indicate that ADAR1 p150 has a positive effect on the levels of miR-376b-3p, whereas ADAR2 decreases levels of both miR-376b-3p and miR-376b-5p.

ADAR2 prevents processing of pri-miR-376b

The ADAR enzymes have previously been shown to affect the processing of different miRNAs, often by affecting the Drosha-mediated generation of pre-miRNAs (20, 21, 32) and the Dicer-mediated cleavage of pre-miRNAs to form mature miRNAs (33, 34). To determine how the ADAR enzymes were affecting miR-376b processing, we analyzed the abundance of pre-miRNA and mature miRNA with Northern blot (Fig. 4*A*). This allowed us to analyze abundance of pre-miRNA as well as mature miRNAs. The probes used for the Northern blot consisted of an equal mix of probes binding unedited and edited forms of the miRNA, in order for editing to not affect efficiency of probe binding. Abundance of pre-miR-376b-3p and mature miR-376b-3p was not significantly different from controls following overexpression with enzymatically active or inactive ADAR1 p110 or p150 (Fig. 4, *B* and *C*). ADAR2 cotransfection, on the other hand, led to clear decreases of both pre-miRNA and mature miRNA abundance in an editing-independent manner. Pre-editing of the 3p +6 site did not

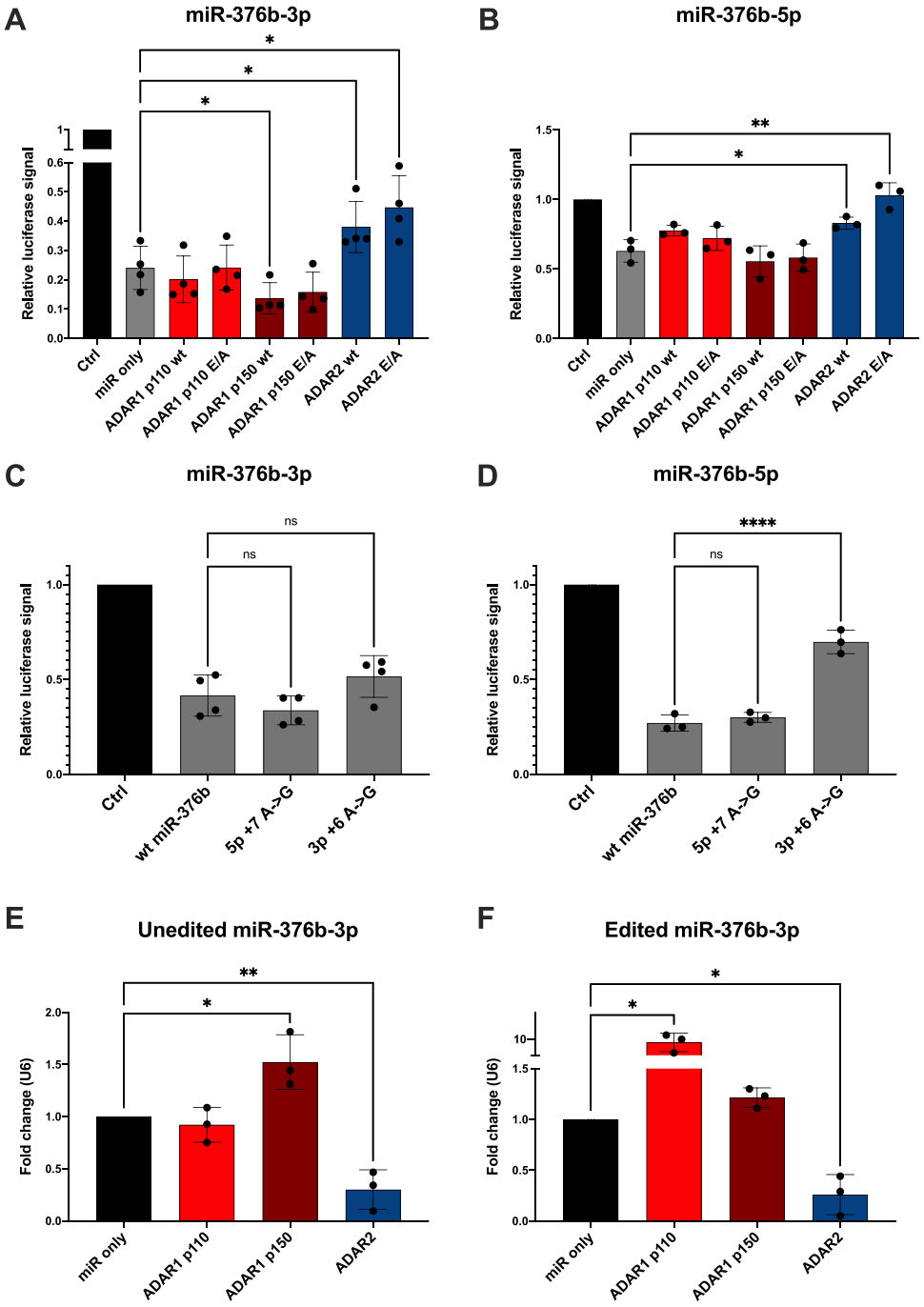

Figure 3. Effects of the ADAR enzymes on the maturation of miR-376b. *A–D*, luciferase reporters of miRNA activity were cotransfected with the miR-376b expression vector and the different forms of the ADAR enzymes. The signal of firefly luciferase containing miRNA-binding sites was normalized to the signal of renilla luciferase generated from the same vector but lacking miRNA-binding sites, and the resulting values were normalized to a control sample without miRNA expression vector. Luciferase assays were performed for miR-376b-3p (*A*) and -5p (*B*) (n = 3). Similarly, the effects of pre-editing the miRNA expression vectors was analyzed using luciferase assays for 3p (*C*) and 5p (*D*) (n = 3). *E* and *F*, miRNA-specific LNA-based qPCR was performed on cotransfections of the miR-376b expression vector and the ADAR enzymes. Primer pairs able to distinguish between the unedited (*E*) and the edited (*F*) forms of miR-376b-3p were used. Expression levels were calculated as ΔΔCt, with normalization to expression of U6 snRNA expression relative to the miR-only control (n = 3). ADAR, adenosine deaminase acting on RNA; LNA, locked nucleic acid.

significantly alter abundance of pre-miRNA or mature miRNA. Surprisingly, pre-editing of the 5p +7 site altered pre-miRNA abundance and processing, with the pre-miRNA at a lower molecular weight and reduced abundance, whereas mature miRNA abundance remained unchanged. In summary, these results further confirm that ADAR2 decreases abundance of both pre-miR-376b-3p and mature miR-376b-3p in an editing-independent manner.

The effect of ADAR2 on the levels of pre-miRNA and mature miRNA could be due to either decreased synthesis of

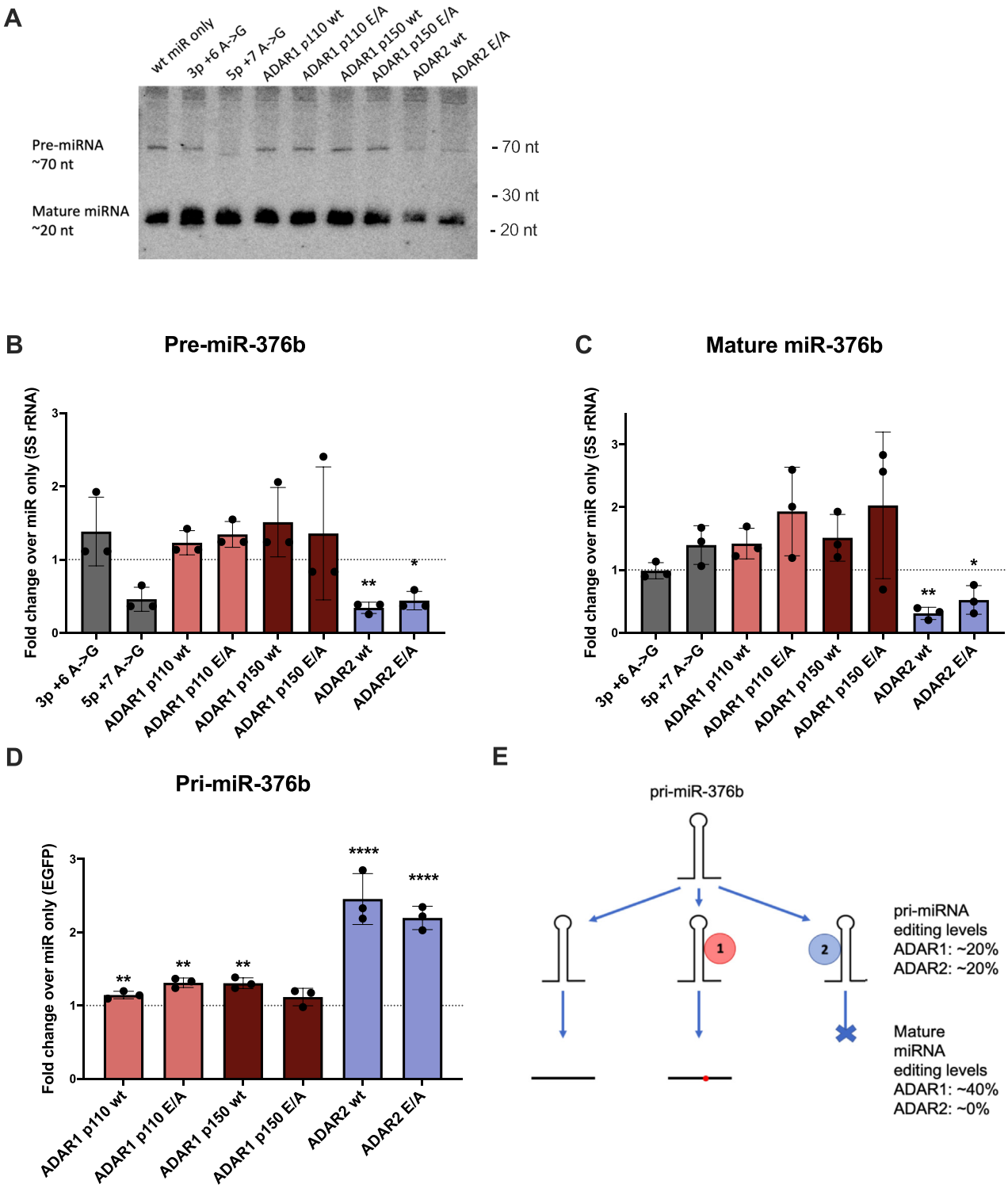

Figure 4. Effects of the ADAR enzymes on the biogenesis of miR-376b. *A*, Northern blot was performed on HEK-293 cells transfected with the miR-376b expression vector (wildtype or pre-edited at the 3p +6 or the 5p +7 sites) and the different forms of the ADAR enzymes. An upper band at about 70 nt corresponded to the pre-miRNA, whereas a lower band at about 20 nt corresponded to mature miRNA. *B* and *C*, quantifications of Northern blots, pre-miR-376b (*B*) and mature miR-376b-3p (*C*). Signals were normalized to the levels of 5S rRNA as observed using ethidium bromide staining of the RNA gels and expressed as relative to miR-only controls (n = 3). *D*, qPCR of pri-miR-376b levels in HEK-293 cells transfected with miRNA expression vector and the different forms of the ADAR enzymes. Cells were also cotransfected with pEGFP, which was used for normalization in order to account for possible differences in transfection efficiency. Expression levels were calculated as ΔΔCt, with normalization to expression of EGFP mRNA, relative to the miR-only control (n = 3). *E*, a model for how the observed editing levels of pri-miR-376b and mature miR-376b can be determined by the effects of the ADAR enzymes. At the pri-miRNA stage, ADAR1 and ADAR2 edit their respective sites at about 20%. ADAR2 will in addition prevent maturation, and because of the competition between the two enzymes, the pool of successfully processed miRNAs will contain an overrepresentation of those that interacted with (and edited by) ADAR1, possibly accounting for the increased editing level observed in the mature miR-376b-3p. ADAR, adenosine deaminase acting on RNA; HEK-293, human embryonic kidney 293 cell line; pEGFP, phosphorylated enhanced GFP; pre-miRNA, precursor miRNA.

pri-miRNA or decreased processing of pri-miRNA. To distinguish between these possibilities, we first performed RT–qPCR using primers positioned in the flanking sequence of the pre-miRNA hairpin to detect unprocessed pri-miRNA transcripts (Fig. 4*D*). Cotransfection with the different forms of ADAR1, except for inactive p150, led to slight but significant increases in pri-miRNA levels, whereas ADAR2 cotransfection led to a more than twofold increase in pri-miR-376b levels. This result indicates that ADAR2 prevents pri-miR-376b processing, leading to an accumulation of pri-miRNA transcripts, resulting in the reduction in miR-376b-3p production. Since ADAR1 and ADAR2 seems to compete for binding to pri-miR-376b and ADAR2 efficiently prevents pri-miRNA processing, mature miR-376b-3p will be enriched for transcripts that interacted with ADAR1. This is supported by the increased ADAR1-mediated editing of mature miR-376b-3p in contrast to the lower editing observed in the pri-miRNA and the low ADAR2-mediated editing of mature miR-376b-5p (Fig. 4*E*). In summary, ADAR2 causes a decrease in pre-miR-376b-3p and mature miR-376b-3p by inhibiting Drosha-mediated processing of pri-miR-376b. Given the competition of the two ADAR enzymes for binding to pri-miR-376b-3p, it is possible that this effect indirectly leads to the higher ADAR1-mediated editing observed in the mature miR-376b-3p.

Edited miR-376b-3p regulates mRNA levels of genes with neuronal function

Next, we investigated the physiological significance of the regulatory mechanisms reported previously. Given that the level of editing of miR-376b-3p is high in the brain but absent when this miRNA is expressed in embryos (28), and that its biogenesis is regulated by brain-enriched ADAR2, we postulated that edited miR-376b-3p regulates the mRNA levels of genes with neuronal function. We generated an *in silico* prediction of targets of edited miR-376b-3p with the custom prediction tool of miRBD (35), replacing the edited adenosine of miR-376b-3p with guanosine in order to mimic the effects of editing. For an initial analysis of editing-mediated miR-376b-3p retargeting, we compared the list generated for unedited miR-376b-3p to predicted targets of pre-edited miR-376b-3p. With a prediction score cutoff of 80, 103 and 84 genes were predicted targets of the unedited and edited miRNAs, respectively, with only one gene shared between the two (Tables S1 and S2). Gene Ontology (GO) term enrichment analyses were performed on the two lists to identify annotated functions of the target genes (Fig. S3). The GO terms for the targets of edited miR-376b-3p included several terms related to neuronal function, such as vesicle docking and negative regulation of neurotransmitter transport, whereas the list for the unedited miR-376b-3p did not include terms related to neuronal function.

From the list of predicted targets of edited miR-376b-3p, we selected four genes with a prediction score higher than 90, annotated neuronal functions, and robust expression in the mouse neuroblastoma cell line Neuro2a (N2a) for experimental verification. The four genes included sphingomyelin synthase 1 (*Sgms1*), transcription factor 12 (*Tcf12*), 4-aminobutyrate aminotransferase (*Abat*), and syntaxin 17 (*Stx17*). First, we transfected N2a cells with the miR-376b-3p miRNA mimics, with or without pre-editing (Fig. 5*A*). Using RT–qPCR, we observed significantly decreased mRNA levels of all four target genes following transfection with pre-edited miR-376b-3p, whereas transfection with the unedited miRNA did not decrease mRNA levels.

To further verify the targeting of these four genes by the edited miR-376b-3p, and to exclude indirect effects, we performed dual luciferase assays where a sequence of the 3′UTR of each target gene containing one or two predicted target sites was inserted into the 3′UTR of firefly luciferase. Cotransfection of the luciferase reporter with the expression vector of the pre-edited, but not the unedited, miR-376b led to decreased luciferase activity for all four genes (Fig. 5*B*). This effect was lost upon specific deletion of the seven nucleotides in the luciferase vector complementary to the seed sequence of the edited miR-376b-3p (Fig. 5*C*). In summary, these results show that edited, but not unedited, miR-376b-3p targets these four genes in a direct manner. Since the four genes are related to neuronal functions, this raises the possibility that editing of miR-376b-3p and ADAR2-mediated modulation of miR-376b-3p maturation are able to influence neuronal function in the brain.

Targeting of ABAT by edited miR-376b-3p is conserved and affects GABA catabolism and cell surface presentation of $GABA_A$ α1

In order to identify targets of edited miR-376b-3p with conserved functional importance, we analyzed targeting conservation between mouse and human. For this purpose, we used the custom prediction tool of miRDB to predict targeting of the human-edited miR-376b-3p and generated a list of predicted targets after substituting the edited adenosine for guanosine (Table S3). As in mouse, we observed *TCF12* and *ABAT* among the top predicted targets, with prediction scores of 97 and 95, respectively. For ABAT, we were able to experimentally verify the targeting of human-edited miR-376b-3p to *ABAT*, by transfecting the human neuroblastoma cell line SH-SY5Y with miR-376b-3p miRNA mimics, and observing a reduction of *ABAT* transcript following transfection with the pre-edited, and not the unedited, miR-376b-3p (Fig. 6*A*).

Since ABAT is the enzyme responsible for the catabolism of the neurotransmitter GABA and could thereby be involved in the regulation of GABAergic signaling, we decided to focus on this target gene. Subsequently, an immunoblot of N2a cells transfected with the miR-376b-3p expression vector confirmed that the reduction of *Abat* transcript by edited miR-376b-3p was concurrent with a significantly decreased protein level (Fig. 6*B*).

Jonathan *et al.* (36) recently developed a genetically encoded fluorescent sensor of GABA, where binding of GABA by the Pf622 protein from *Pseudomonas fluorescens* restores the fluorescence of a circularly permuted GFP. By cotransfecting

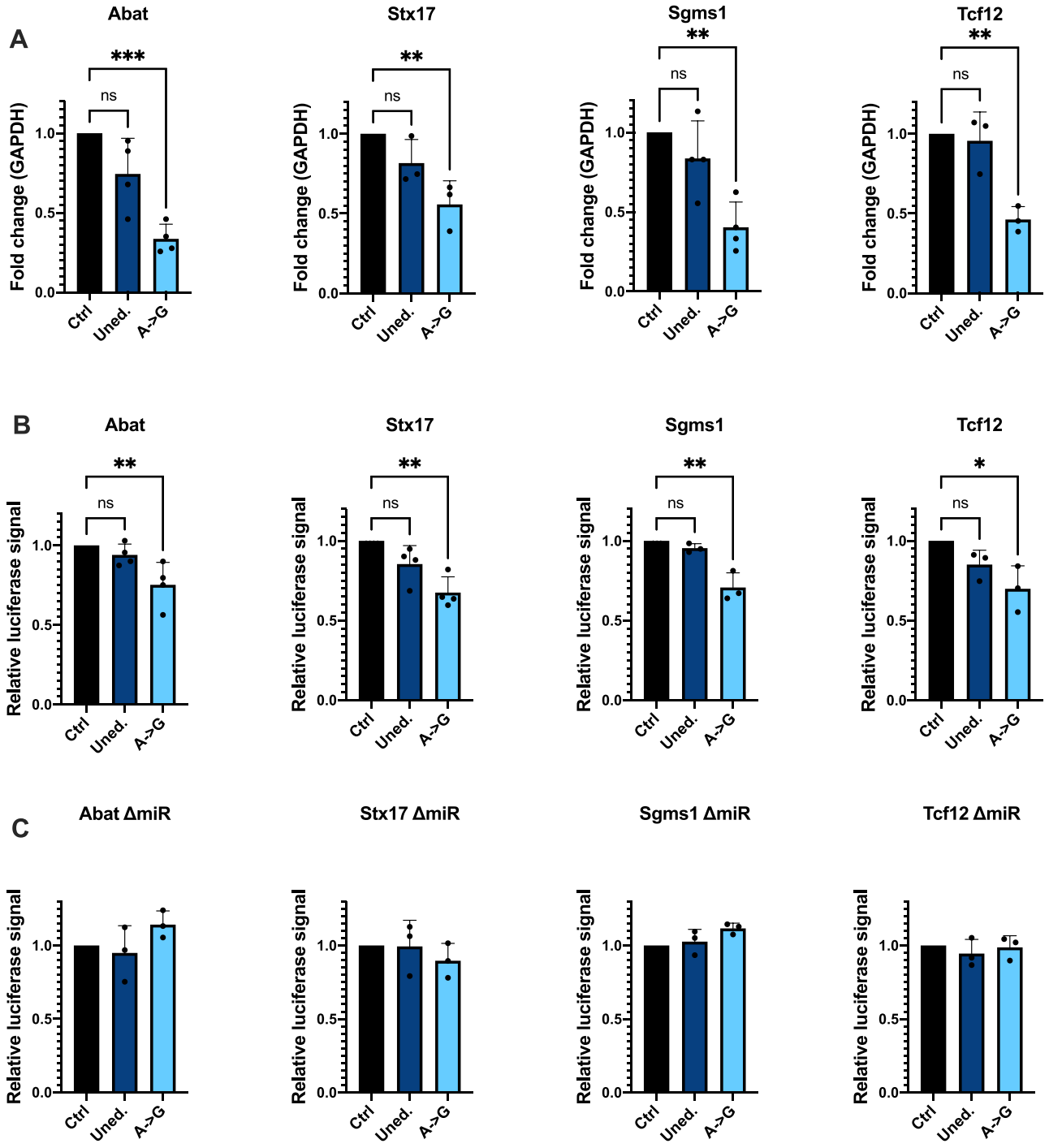

Figure 5. Neuronal targets of edited miR-376b-3p. *A*, N2a cells were transfected with miRNA mimics whereupon RT–qPCR was performed on four putative target transcripts (*Abat*, *Stx17*, *Sgms1*, and *Tcf12*). A nonspecific control miRNA mimic (ctrl) was compared with miRNA mimics for unedited miR-376b-3p (uned.) and pre-edited miR-376b-3p (A->G). Expression levels were calculated as ΔΔCt, with normalization to expression of GAPDH relative to the miR-only control (n = 3). *B*, luciferase assays were performed where the firefly luciferase transcript contained sequences from the 3′UTRs of the putative target genes. HEK-293 cells were transfected with the luciferase reporters and the miRNA expression vector, either unedited (uned.) or pre-edited (A->G). The signal from firefly luciferase was normalized to renilla luciferase signal, and expression was normalized to the control samples (n = 3). *C*, luciferase assay was repeated following the specific deletions of nucleotides complementary to the miR-376b-3p seed sequence (n = 3). HEK-293, human embryonic kidney 293 cell line; N2a, Neuro2a; qPCR, quantitative PCR.

this iGABASnFR vector with an miRNA mimic of pre-edited miR-376b-3p, we observed an increased level of fluorescence as measured by fluorescence-activated cell sorting (Fig. 6*C*). This result indicates that the downregulation of ABAT following transfection by pre-edited miR-376b-3p leads to increased intracellular levels of GABA because of decreased GABA catabolism.

Altered levels of intracellular GABA could affect the levels of GABA in synaptic vesicles of GABAergic synapses. In addition, it has been observed that intracellular GABA acts as a

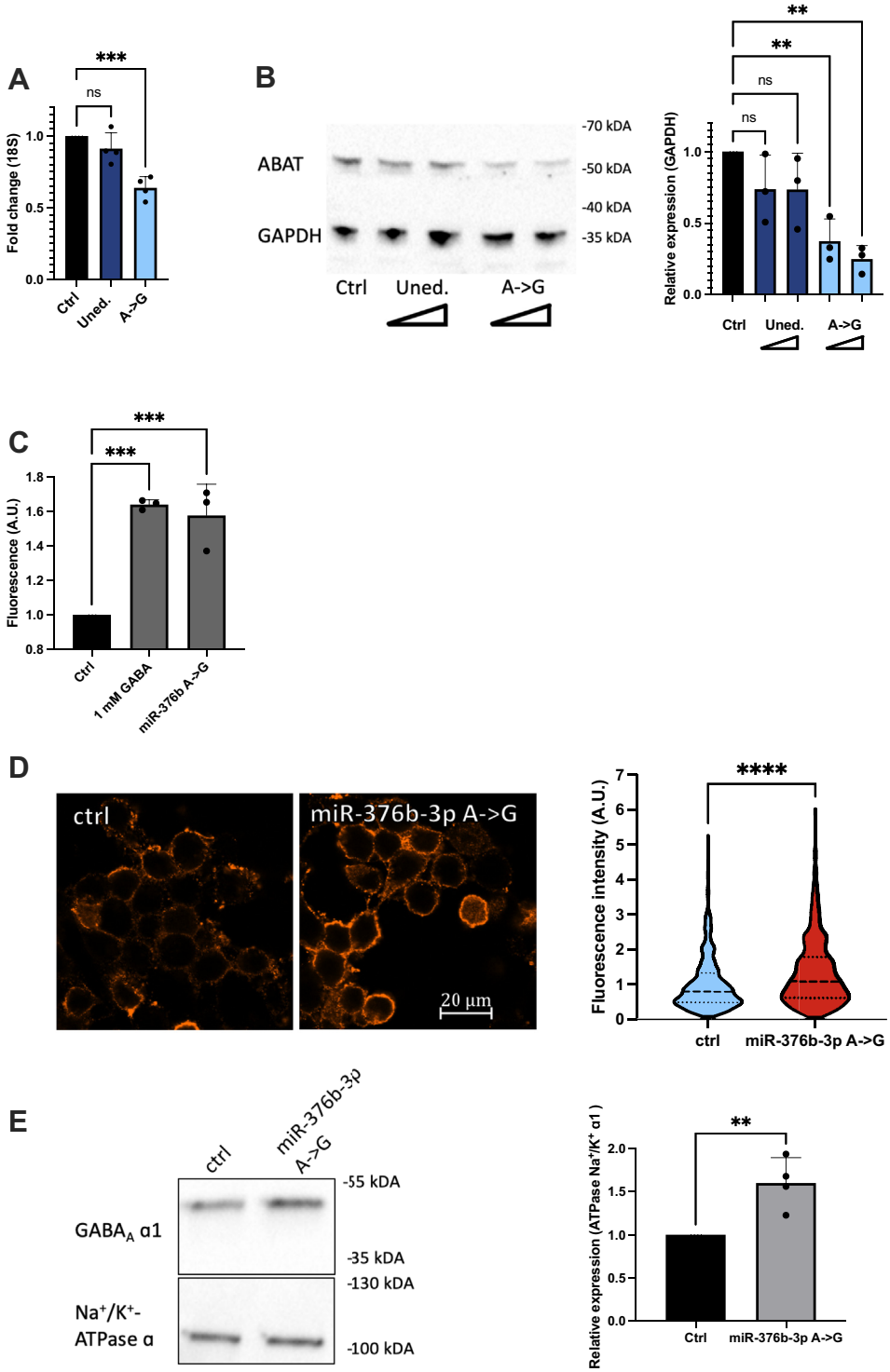

Figure 6. Targeting of Abat by edited miR-376b-3p is conserved and possibly regulates GABAergic signaling. *A*, human glioblastoma SHSY-5Y cells were transfected with miRNA mimics, whereupon qPCR of Abat transcript was performed. A nonspecific control miRNA mimic (ctrl) was compared with miRNA mimics for unedited miR-376b-3p (uned.) and pre-edited miR-376b-3p (A->G). Expression levels were calculated as ΔΔCt, with normalization to expression of 18S rRNA relative to the miR-only control (n = 3). *B*, immunoblot of N2a cells transfected with two different amounts of miR-376b expression vectors, either unedited (uned.) or pre-edited (A->G). Expression of ABAT was normalized to GAPDH expression and compared with a control transfection (ctrl) (n = 3). *C*, N2a cells were transfected with the fluorescent GABA sensor iGABASnFR and cotransfected with either a nonspecific control miRNA mimic or pre-edited miR-376b-3p mimic. Cells were grown in 1 mM GABA to verify the efficacy of the assay. FACS was used to determine total fluorescence from the samples, with values normalized to control (n = 3). *D*, N2a cells transfected with $GABA_A$ receptor subunits α_1, β_2, and γ_2L whereupon immunofluorescence of nonpermeabilized cells was performed using anti-$GABA_A$ α_1 antibodies. The IntDen function of ImageJ was used to measure fluorescence intensity, and values were normalized to the average of the control samples of each experiment. *E*, N2a cells transfected with $GABA_A$ receptor subunits α_1, β_2, and γ_2L and either a nonspecific control miRNA mimic or pre-edited miR-376b-3p mimic whereupon cell surface protein biotinylation was performed, followed by isolation of biotinylated proteins and immunoblot using anti-$GABA_A$ α_1 antibodies. $GABA_A$ α_1 cell surface expression was normalized to Na^+/K^+-ATPase α (n = 4). Abat, 4-aminobutyrate aminotransferase; FACS, fluorescence-activated cell sorting; GABA, gamma aminobutyric acid; $GABA_A$, GABA type A; N2a, Neuro2a; qPCR, quantitative PCR.

ligand chaperone in the secretory pathway for the cell surface expression of $GABA_A$ receptors, where increased levels of intracellular GABA resulted in increased numbers of $GABA_A$ receptors on the cell surface (37, 38). This would imply that increased levels of intracellular GABA as a result from expression of edited miR-376b-3p could increase the number of $GABA_A$ receptors on the cell surface by this mechanism. To investigate this possibility, we transfected N2a cells with the $GABA_A$ receptor subunits α_1, β_2, and γ_2L and performed immunofluorescence of unpermeabilized cells with anti-$GABA_A$ α_1 antibodies. We observed a clear membrane-localized fluorescence (Fig. 6*D*). Upon cotransfection with miRNA mimics for edited miR-376b-3p, we observed significantly increased surface fluorescence. In addition, we performed a cell surface protein biotinylation and purification experiment in order to enrich for proteins on the cell surface. Upon performing an immunoblot on the purified membrane proteins, we observed increased levels of $GABA_A$ α_1 following cotransfection with miRNA mimics for edited miR-376b-3p (Fig. 6*E*). This increase was not observed for the total protein levels of $GABA_A$ α_1 (Fig. S4), indicating increased surface presentation of $GABA_A$ receptors but not increased $GABA_A$ total protein levels. In summary, these results suggest that the reduction of ABAT levels mediated by edited miR-376b-3p leads to increased intracellular GABA concentration and increased $GABA_A$ receptor cell surface expression.

Discussion

By having multiple genes within one transcript, such as the genes of prokaryotic polycistronic mRNAs and the eukaryotic miRNA clusters, means that transcriptional regulation is shared and enables coordination and synchronicity of gene expression. This is important for regulating genes with shared biological functions: members of the same pathway or genes involved with establishing a particular cellular state, for example. In the case of the miR-379–410 cluster, expressed in both early embryonic development and in the adult brain, an interesting challenge is posed. How can the same 39 miRNA genes function in two such different biological contexts? The answer is likely to be post-transcriptional modulation of miRNA expression. Despite the fact that the miRNAs of the cluster share transcriptional regulation, the expression patterns of the individual miRNAs differ between embryonic tissues and adult brain (13). Furthermore, high levels of A-to-I editing of members of the cluster, specific to brain tissue, enable redirection of miRNAs in a tissue-specific manner. Our study, and others (20, 21, 28), show that the ADAR enzymes are able to affect the expression of members of the miR-379–410 cluster in diverse ways, specific to particular miRNAs. Given that ADAR expression and activity can vary greatly in different tissues and developmental stages (25, 27, 39), this provides a mechanism for modulating the expression of members of the miR-379–410 cluster as required for various biological contexts. In addition, ADAR expression and activity varies between different brain regions and neural cell types (25, 40, 41), and thereby ADAR-mediated modulation of miRNA expression provides a regulatory mechanism for generating the complex transcriptional landscape of the brain.

In this study, we observe that levels of edited miR-376b-3p increase during brain development, without a corresponding increase in either the expression of unedited miR-376b-3p or in the editing level of pri-miR-376b, consistent with relatively stable ADAR1 expression during brain development (29, 39, 41). One explanation for this observation could be altered biogenesis of miR-376b-3p during development, with a mechanism that affects the generation of edited and unedited miRNA differently. Here, we demonstrate that ADAR2 inhibits the processing of pri-miR-376b. Furthermore, our observations indicate competitive binding by ADAR1 and ADAR2 to pri-miR-376b, in agreement with previous reports that miR-376b-3p +6 editing is increased in the $ADAR2^{-/-}$ mouse (27). Together, this likely results in the enrichment of ADAR1-edited miR-376b-3p compared with the editing level observed in the pri-miRNA. ADAR2-mediated inhibition of Drosha processing could then be the explanation for the specific increase of the edited form of miR-376b-3p during development. An increased nuclear accumulation of ADAR2 in neurons (29) coupled to an increased expression of pri-miR-376b would lead to an increase in the edited form (where the miRNA interacted with ADAR1) but not the unedited form (where the miRNA was more likely to interact with ADAR2, inhibiting its biogenesis). In support of this proposal, the increase in levels of edited miR-376b-3p was found to be coupled to an increase in the editing of the ADAR2-mediated 5p +7 site.

While the inhibitory effect of ADAR2 is quite clear and consistent in this study, a possible effect of ADAR1 on miR-376b levels is less so, with some experiments indicating a positive effect, whereas others did not show this. Such a positive effect could for example be reflecting the previously observed increased pre-miRNA processing by Dicer when in complex with ADAR1 (34), especially for the more cytoplasmic p150 isoform (Fig. 3*E*). A possible positive effect of ADAR1 on miR-367b maturation could contribute to the inhibitory effect of ADAR2, given that they compete for pri-miRNA hairpin binding. Such coordination and competition between editing mediated by the two ADAR enzymes has been reported previously to occur on a large scale (42). The inability of ADAR2 to prevent editing by ADAR1 p150 could possibly reflect the cytoplasmic nature of p150 and that it performs editing of unprocessed pri-miR-376b in the cytoplasm, whereas ADAR2 is strictly nuclear and can therefore not compete efficiently with this editing. As ADAR2 decreases both pre-miRNA and mature miRNA while causing an accumulation of pri-miRNA, the results indicate that ADAR2 is able to prevent processing by Drosha, as has been shown for other miRNAs (20, 21, 32). It seems likely that the abilities of ADAR2 to block both ADAR1 editing and Drosha processing of miR-376b are related and reflect the nature of the interaction between ADAR2 and the miRNA. Possibly, ADAR2 forms a stronger and more stable interaction with the miRNA hairpin and thereby prevents access by other factors, and future studies to test the affinity of ADAR2 for pri-miR-376b could confirm this. According to

this hypothesis, the affinity would be much higher than the affinity of ADAR1.

While the inhibitory effect of ADAR2 is editing independent, we did observe a reduction in miR-376b-5p activity following pre-editing of the ADAR2-mediated 5p +7 site, which raises the possibility that a separate editing-dependent effect contributes to modulate miR-367b expression. Editing at this site will lead to the formation of an I–C base pair, thereby increasing the complementarity of the miRNA hairpin. This could possibly affect strand selection, the mechanism by which one of the mature miRNAs is incorporated into the RISC, whereas the other is degraded, as the strand with the weakest complementarity at its 5′-end is more likely to become incorporated into the RISC (43, 44). However, pre-editing the 5p +7 site does not increase miR-376b-3p activity, which would be the result of a shift in strand selection. Another possibility is that the increased complementarity resulting from pre-editing the 5p +7 site leads to slicing of the 5p passenger strand (45, 46), thereby decreasing miR-376b-5p activity.

miRNA editing has previously been observed to redirect miRNAs to target genes associated with neuronal functions, statistically (26). Non-neuronal miRNA editing is almost absent in mice, whereas in humans, miRNA editing is found in certain other tissues such as the vascular endothelium (47) where miRNA editing retargets miRNAs to transcripts involved in organ development (26). This implies a more recent evolutionary development of expanding the role of miRNA editing, possibly contributing to the higher complexity of the human brain. miR-376b-3p specifically is not only highly conserved between mouse and human, but its seed sequence, which is unique in mouse, is shared with two other miRNAs in humans: miR-376a1 and miR-376a2 (48). This supports the importance of this miRNA, which not only is conserved in humans but also expanded upon. Since *Abat* is a conserved target between mouse and humans, it is possible that regulation of GABAergic signaling *via Abat* has gained further importance in the human lineage. Further supporting a connection between edited miR-376b-3p and GABAergic signaling is the observation that *Shisa7*, a regulator of $GABA_A$ receptor function, is also targeted by edited miR-376b-3p (Fig. S5). In fact, Shisa7 is the top-ranked gene in the list of predicted targets for the human-edited miR-376b (Table S3). A role in regulation of GABAergic signaling by members of the miR-379–410 cluster is supported by the phenotype of mice lacking the miRNA cluster, as lack of GABAergic inhibitory signaling could contribute to the observed hypersociality and enhanced anxiety-related behaviors (10, 12). While this study focused on the upregulation of genes involved in glutaminergic signaling, genes involved in GABAergic signaling were found to be downregulated (12), which supports the idea that miRNA-mediated downregulation of *Abat* is part of a regulatory network that increases GABAergic signaling. While the physiological importance of the results presented in this study is yet to be determined, here we propose a functional connection between ADAR-mediated regulation of an miRNA and modulation of GABAergic signaling.

Experimental procedures

Animals and cell culture

NMRI mice were obtained from Charles River Laboratories and Nova-SCB. All animal procedures were approved by the Animal Ethics Committee of the North Stockholm region. HEK-293, N2a, and SHSY-5Y cells were grown in Dulbecco's modified Eagle's medium (Life Technologies) containing 10% fetal bovine serum (Life Technologies) and 100 U/ml penicillin/streptomycin. Cells were kept at 37 °C in an incubator with 5% CO2.

Pri-miRNA sequencing

Total RNA was isolated from 6- to 8-week-old mouse brains with TRIzol (Invitrogen) according to the manufacturer's instructions. To remove genomic DNA contamination prior to complementary DNA (cDNA) synthesis, the total RNA was treated with Amplification Grade DNase I kit (Sigma). Gene-specific first-strand cDNA synthesis was performed using SuperScriptIII (Thermo Fisher Scientific) and seven primers 50 to 100 bp downstream of the seven pri-miRNA genes. Samples were treated with RNAse A (Thermo Fisher Scientific) in order to degrade RNA, followed by second-strand cDNA synthesis using Platinum Taq (Thermo Fisher Scientific) and seven primers 50 to 100 bp upstream of the seven pri-miRNA genes. Samples were then treated with S1 Nuclease (Thermo Fisher Scientific) in order to degrade single-stranded DNA, followed by PCR clean-up using NucleoSpin Gel and PCR clean-up (Macherey–Nagel). The double-stranded cDNA was end-repaired, A-tailed, and then ligated to TruSeq single index adapters using TruSeq Stranded mRNA Library Prep kit (Illumina) and following the manufacturer's protocol. The cDNA libraries were PCR amplified by 15 cycles. The libraries were validated using Bioanalyzer DNA 1000 assay kit (Agilent) and measured with Qubit dsDNA HS Assay Kit (Invitrogen) prior to pooling and sequencing. The 80 bp paired-end sequencing was carried out using the Illumina NextSeq 500 and the NextSeq 500 High Output sequencing kit (Illumina).

Small RNA-Seq

RNA samples were obtained as described previously. Small RNA-Seq was performed by the Swedish National Genomic Infrastructure facilities using the TruSeq small RNA kit and sequenced on an Illumina NextSeq 550 machine. Briefly, the quality of total RNA and small RNA fragments was evaluated by bioanalyzer (Agilent), and samples were delivered following the recommendations of the National Genomic Infrastructure facility. Library preparation and sequencing were carried out according to their standard procedures.

RNA variant calling for pri-miRNA and small RNA-Seq

RNA-Seq variant calling analysis was performed following the Genome Analysis Toolkit recommendations for RNA-Seq short variant discovery. FASTQ files were aligned to mm10 reference genome using STAR (2.5.3a) software using two-pass mode. BAM files were processed using picard-tools (2.23.4) software to

further perform variant calling analysis using HaplotypeCaller (Genome Analysis Toolkit, version 4.1.8.1). Called edited sites were filtered and restricted to chr12 for those transitions associated with RNA editing events. Variant calling for small RNA-Seq was performed using REDitools (49) (version 1.2.1) software. Briefly, FASTQ files were trimmed using Trim-galore (Babraham Bioinformatics, version 0.6.5) and aligned using Bowtie2 (50) (version 2.2.6) software against mm10 reference genome. BAM files were processed and sorted using samtools (version 1.9) to finally perform the variant calling using REDItools (version 1.2.1), restricting the analysis to A > G and T > C transitions on those reads aligned to chr12. Raw data are publicly available at the National Center for Biotechnology Information BioProject database, ID PRJNA768781.

Constructs

Pri-miRNA constructs

A roughly 500-nucleotide-long sequence of mmu-pri-mir-376b was PCR amplified from mouse DNA and cloned into pcDNA3. The change from A to G at editing site in miR-376b-5p position +7 and −3p position +6 was accomplished by QuikChange site-directed mutagenesis (Stratagene) according to the manufacturer's instructions.

miRNA activity reporter constructs

miR-376b-5p and miR-376b-3p, with and without complementarity to pre-edited miRNA, reporter constructs were made by inserting synthetic DNA fragments (IDT) into the SalI cloning site of pmirGLO Dual-Luciferase miRNA Target Expression Vector (Promega). The sequences consist of three perfectly complementary miRNA-binding sites. For luciferase vectors to assay miRNA targeting of Abat, Sxt17, Sgms1, and Tcf12, sequences from the 3′UTRs containing either one or two predicted miRNA-binding sites were either cloned by PCR or synthesized (IDT) and inserted into the pmirGLO vector as described previously. Predicted miRNA target sites were either deleted from the sequence before DNA synthesis or removed using QuikChange site-directed mutagenesis (Stratagene) according to the manufacturer's instructions

Protein expression vectors

Expression vectors for mouse ADAR1 and ADAR2 were generated by PCR amplification of the ORFs of the genes from mouse DNA. The PCR products were subsequently cloned into pcDNA3. For the inactivating point mutations, QuikChange site-directed mutagenesis (Stratagene) was used according to the manufacturer's instructions (ADAR1 E861A and ADAR2 E396A) (30, 31). Expression vectors for murine $GABA_A$ receptor subunits α_1, β_2, and γ_2L in the plasmid backbone pRK5 were a gift from Trevor Smart (University College London).

Transfection

HEK-293, N2a, and SHSY-5Y cells were transfected in 6-well plates (Northern blot and microscopy), 12-well plates (RT–PCR, qPCR, or fluorescence-activated cell sorting), 48-well plates (Dual luciferase assay), or 10 cm dishes (biotinylation assay) using Lipofectamine 2000 reagent (Invitrogen) following the manufacturer's instruction. After 48 h, cells were washed with PBS and lysed according to subsequent experimental procedures.

Dual luciferase reporter assay

Transfected cells were washed in PBS and lysed for luciferase measurements using the Dual Luciferase assay kit from Promega. Luciferase activity was measured using Orion II Microplate Luminometer (Berthold Detection System).

RNA extraction, RT–qPCR, RT–PCR, and Sanger sequencing

RNA extraction and cDNA synthesis

Total RNA was isolated from mouse brain or transfected cells with TRIzol (Invitrogen) according to the manufacturer's instructions. To remove genomic DNA contamination prior to cDNA synthesis, the total RNA was treated with Amplification Grade DNase I kit (Sigma). DNase-treated RNA was reverse transcribed with SuperScript II and random hexamers (Invitrogen).

qPCR of pri-miRNA and mRNA

For pri-miR-376b and predicted target genes, qPCR was performed with KAPA SYBR FAST (Sigma–Aldrich) qPCR reagent in a Rotor-Gene Q machine (Qiagen). For qPCR of pri-miR-376b, cotransfected pEGFP C1 (Clontech) was used for normalization with the ΔΔCt method.

qPCR of mature miR-376b-3p

First-stranded cDNA synthesis was performed with miRCURY LNA RT Kit (Qiagen). Customer representatives of Qiagen assisted in the design of LNA PCR primers specific for either unedited or edited miR-376b-3p. The specificity of the primers was tested with either unedited or pre-edited miR-376b expression vectors transfected in HEK-293 cells. qPCR was performed with miRCURY LNA SYBR Green PCR Kit (Qiagen) in a Rotor-Gene Q machine (Qiagen).

RT–PCR and Sanger sequencing

For editing analysis of transcript from pri-miR-376b expression vectors, RT–PCR was performed with one vector-specific and one insert-specific primer and high-fidelity DNA polymerase (Thermo Fisher Scientific). For endogenous pri-miR-376b transcripts from mouse brain, primers about 100 nt upstream and downstream of the pri-miRNA hairpin were used for amplification. Editing frequencies in pri-miRNAs was determined by measuring the ratio between the A and the G peak height in Sanger sequencing (Eurofins Genomics) chromatograms of gel-purified RT–PCR amplicons. The percentage of editing was calculated as the peak height of G/(A + G) × 100.

Northern blot

About 20 μg of total RNA from transfected HEK-293 cells was loaded in a 15% PAGE 8.75 M urea gel in a Mini-Protean system (Bio-Rad). The RNA was then transferred to a Zeta Probe GT Nylon+ membrane (Bio-Rad), which was blocked, washed, and hybridized with the probes according to the manufacturer's instructions. Probes consisted of DNA sequences complementary to the full length of mature miR-376b, with a 1:1 mix of probes complementary to unedited and edited miR-376b. Probes were labeled with γ-ATP (PerkinElmer) with T4 Kinase (Invitrogen). The sizes of the resulting bands were verified by electrophoresis next to the Ambion Decade Marker (Thermo Fisher Scientific). The Northern blots were visualized with an FLA-3000 phosphorimager (Fujifilm), and their density was measured. All experiments were performed in triplicate.

GO enrichment analysis

GO enrichment analysis was performed with Cytoscape (version 3.7.1) (51) and ClueGO (version 2.5.4) (52) software. Briefly, gene targets list from either edited or not edited miRNA were submitted to ClueGO software ontology enrichment analysis using the biological process ontology classification (vBP_EBI_UniProt_GOA_27.02.2019). Only statistically significant groups were displayed, with a Bonferroni step-down multiple comparison post hoc test. A corrected $p < 0.05$ was considered statistically significant.

Immunoblot and cell surface protein biotinylation assay

For expression of immunoblots, transfected cells were lysed with cOmplete Lysis-M containing cOmplete Protease Inhibitor Cocktail (Sigma–Aldrich). Total protein concentration was determined with Bradford assay, and samples were separated on 4 to 15% SDS-polyacrylamide gels (Bio-Rad) and blotted onto polyvinylidene fluoride membranes. The ABAT protein level blots were probed with the following primary antibodies overnight at 4 °C: 1:750 anti-ABAT (catalog no.: EPR20842; Abcam) and 1:10,000 anti-GAPDH (catalog no.: ab8245; Abcam). ADAR protein level blots were probed with the following primary antibodies overnight at 4 °C: 1:500 anti-ADAR1 (catalog no.: sc-73408; Santa Cruz Biotechnology), 1:500 anti-ADAR2 (catalog no.: HPA018277; Sigma–Aldrich), and 1:40,000 anti-β-actin (catalog no.: A1978; Sigma–Aldrich).

For isolation of cell surface proteins, Pierce Cell Surface Biotinylation and Isolation Kit (Thermo Fisher Scientific) was used on transfected N2a cells according to the manufacturer's instructions. An immunoblot was performed on the protein extracts as described previously, as well as total protein isolated with radioimmunoprecipitation assay buffer, using 1:750 anti-$GABA_A$ receptor alpha 1 antibody (catalog no.: ab33299; Abcam) and 1:1000 anti-ATP1A1/ATP1A2/ATP1A3 (catalog no.: sc-48345; Santa Cruz). Horseradish peroxidase–conjugated secondary antibodies (DAKO) were used at a 1:5000 dilution. Chemiluminescent detection of protein was performed with the WesternBright Sirius detection system (Advansta), and band intensities were quantified with Image-Lab (Bio-Rad).

Flow cytometry

In order to indirectly measure changes in intracellular GABA, N2a cells were transfected with a low amount of pAAV.hSynap.iGABASnFR (catalog no.: 112159; Addgene). As a positive control, cells were grown in media supplemented with 1 mM GABA (Sigma–Aldrich). Cells from each well from a transfected 12-well plate were resuspended in 1 ml PBS, followed by a dilution of between 1:10 and 1:50, depending on the experiment. Total fluorescence with a 50 mW 488 nm laser and a green filter (525/30) was measured with a Guava easyCyte 5HT instrument (Millipore). Each sample was represented by three technical replicates, and each replicate was measured for at least 1000 events, following gating for single cells.

Immunofluorescence and image analysis

N2a cells transfected with $GABA_A$ receptor subunits α_1, β_2, and γ_2L were grown on glass slides, washed in PBS, and fixed in 4% paraformaldehyde. After blocking with 3% bovine serum albumin, slides were incubated with 1:750 anti-$GABA_A$ receptor alpha 1 antibody (catalog no.: ab33299; Abcam) overnight at 4 °C. The slides were then incubated with 1:1000 anti-rabbit-IgG conjugated to Alexa-Fluor-546 and mounted with Prolong Gold antifade reagent containing 4′,6-diamidino-2-phenylindole (Invitrogen). For each sample, three or four randomly positioned pictures were taken with an LSM800 confocal microscope (Zeiss). The pictures were then processed with ImageJ, using the subtract background function with a rolling ball radius of 50 pixels. For each sample, at least a 100 cells were quantified with the freehand selection tool and the IntDen function for quantifying signal intensity. For each experiment, the average fluorescence intensity per cell was calculated for control samples and used for normalization.

Statistical analysis

All data were presented as mean ± standard deviation, and p value was analyzed by Student's t test or ANOVA. Values of $p < 0.05$ were considered statistically significant. $^{*}p < 0.05$; $^{**}p < 0.01$; $^{***}p < 0.001$; and $^{****}p < 0.0001$.

Data availability

All the data are contained within the article. Raw sequencing data are publicly available at the National Center for Biotechnology Information BioProject database, ID PRJNA768781.

Supporting information—This article contains supporting information.

Acknowledgments—We thank Dr Neus Visa for feedback on the project and critical reading of the article, Dr Lukas Habernig for his help with fluorescence-activated cell sorting experiments, and Dr

Lars Wieslander for his help setting up Northern blot experiments. We acknowledge support from the National Genomics Infrastructure in Stockholm funded by Science for Life Laboratory, the Knut and Alice Wallenberg Foundation and the Swedish Research Council, and Swedish National Infrastructure for Computing/Uppsala Multidisciplinary Center for Advanced Computational Science for assistance with massively parallel sequencing and access to the UPPMAX computational infrastructure.

Author contributions—A. W., E. A. S., V. K., M. B., C. D., and M. Ö. conceptualization; A. W., M. B., and I. B. methodology; V. K. validation; E. A. S. formal analysis; A. W., V. K., M. B., and I. B. investigation; A. W. writing–original draft; V. K. and M. B. writing–review & editing; A. W. and E. A. S. visualization; E. A. S., M. R. F., C. D., and M. Ö. supervision; M. R. F., C. D., and M. Ö. project administration; M. R. F. and M. Ö. funding acquisition.

Funding and additional information—M. Ö. has been supported by grant from the Swedish Research Council (grant no.: 2018-03823). I. B. and M. R. F. acknowledge the following funding sources: European Research Council starting grant (grant no.: 758397), "miRCell"; Swedish Research Council (grant no.: 2015-04611), "MapToCleave"; and funding from the Strategic Research Area (SFO) program of the Swedish Research Council through Stockholm University.

Conflict of interest—The authors declare that they have no conflicts of interest with the contents of this article.

Abbreviations—The abbreviations used are: *Abat*, 4-aminobutyrate aminotransferase; ADAR, adenosine deaminase acting on RNA; A-to-I, adenosine-to-inosine; cDNA, complementary DNA; GABA, gamma aminobutyric acid; $GABA_A$, GABA type A; GO, Gene Ontology; HEK-293, human embryonic kidney 293 cell line; LNA, locked nucleic acid; N2a, Neuro2a; pre-miRNA, precursor miRNA; pri-miRNA, primary-miRNA; qPCR, quantitative PCR; RISC, RNA-induced silencing complex; *Sgms1*, sphingomyelin synthase 1; *Stx17*, syntaxin 17; *Tcf12*, transcription factor 12.

References

1. Jonas, S., and Izaurralde, E. (2015) Towards a molecular understanding of microRNA-mediated gene silencing. *Nat. Rev. Genet.* **16**, 421–433
2. Denli, A. M., Tops, B. B. J., Plasterk, R. H. A., Ketting, R. F., and Hannon, G. J. (2004) Processing of primary microRNAs by the microprocessor complex. *Nature* **432**, 231–235
3. Zhang, H., Kolb, F. A., Jaskiewicz, L., Westhof, E., and Filipowicz, W. (2004) Single processing center models for human Dicer and bacterial RNase III. *Cell* **118**, 57–68
4. Lewis, B. P., Burge, C. B., and Bartel, D. P. (2005) Conserved seed pairing, often flanked by adenosines, indicates that thousands of human genes are microRNA targets. *Cell* **120**, 15–20
5. Altuvia, Y., Landgraf, P., Lithwick, G., Elefant, N., Pfeffer, S., Aravin, A., Brownstein, M. J., Tuschl, T., and Margalit, H. (2005) Clustering and conservation patterns of human microRNAs. *Nucleic Acids Res.* **33**, 2697–2706
6. Baskerville, S., and Bartel, D. P. (2005) Microarray profiling of microRNAs reveals frequent coexpression with neighboring miRNAs and host genes. *RNA* **11**, 241–247
7. Wang, J., Haubrock, M., Cao, K.-M., Hua, X., Zhang, C.-Y., Wingender, E., and Li, J. (2011) Regulatory coordination of clustered microRNAs based on microRNA-transcription factor regulatory network. *BMC Syst. Biol.* **5**, 199
8. Michlewski, G., and Cáceres, J. F. (2019) Post-transcriptional control of miRNA biogenesis. *RNA* **25**, 1–16
9. Seitz, H., Royo, H., Bortolin, M.-L., Lin, S.-P., Ferguson-Smith, A. C., and Cavaillé, J. (2004) A large imprinted microRNA gene cluster at the mouse Dlk1-Gtl2 domain. *Genome Res.* **14**, 1741–1748
10. Marty, V., Labialle, S., Bortolin-Cavaillé, M.-L., Ferreira De Medeiros, G., Moisan, M.-P., Florian, C., and Cavaillé, J. (2016) Deletion of the miR-379/miR-410 gene cluster at the imprinted Dlk1-Dio3 locus enhances anxiety-related behaviour. *Hum. Mol. Genet.* **25**, 728–739
11. Labialle, S., Marty, V., Bortolin-Cavaillé, M.-L., Hoareau-Osman, M., Pradère, J.-P., Valet, P., Martin, P. G. P., and Cavaillé, J. (2014) The miR-379/miR-410 cluster at the imprinted Dlk1-Dio3 domain controls neonatal metabolic adaptation. *EMBO J.* **33**, 2216–2230
12. Lackinger, M., Sungur, A.Ö., Daswani, R., Soutschek, M., Bicker, S., Stemmler, L., Wüst, T., Fiore, R., Dieterich, C., Schwarting, R. K., Wöhr, M., and Schratt, G. (2019) A placental mammal-specific microRNA cluster acts as a natural brake for sociability in mice. *EMBO Rep.* **20**, e46429
13. Whipple, A. J., Breton-Provencher, V., Jacobs, H. N., Chitta, U. K., Sur, M., and Sharp, P. A. (2020) Imprinted maternally-expressed microRNAs antagonize paternally-driven gene programs in neurons. *Mol. Cell* **78**, 85–95.e8
14. Winter, J. (2015) MicroRNAs of the miR379–410 cluster: New players in embryonic neurogenesis and regulators of neuronal function. *Neurogenesis (Austin)* **2**, e1004970
15. Kawahara, Y., Zinshteyn, B., Sethupathy, P., Iizasa, H., Hatzigeorgiou, A. G., and Nishikura, K. (2007) Redirection of silencing targets by adenosine-to-inosine editing of miRNAs. *Science* **315**, 1137–1140
16. Alon, S., Mor, E., Vigneault, F., Church, G. M., Locatelli, F., Galeano, F., Gallo, A., Shomron, N., and Eisenberg, E. (2012) Systematic identification of edited microRNAs in the human brain. *Genome Res.* **22**, 1533–1540
17. Tian, S., Terai, G., Kobayashi, Y., Kimura, Y., Abe, H., Asai, K., and Ui-Tei, K. (2019) A robust model for quantitative prediction of the silencing efficacy of wild-type and A-to-I edited miRNAs. *RNA Biol.* **17**, 264–280
18. Kume, H., Hino, K., Galipon, J., and Ui-Tei, K. (2014) A-to-I editing in the miRNA seed region regulates target mRNA selection and silencing efficiency. *Nucleic Acids Res.* **42**, 10050–10060
19. Kawahara, Y., Megraw, M., Kreider, E., Iizasa, H., Valente, L., Hatzigeorgiou, A. G., and Nishikura, K. (2008) Frequency and fate of microRNA editing in human brain. *Nucleic Acids Res.* **36**, 5270–5280
20. Vesely, C., Tauber, S., Sedlazeck, F. J., Tajaddod, M., von Haeseler, A., and Jantsch, M. F. (2014) ADAR2 induces reproducible changes in sequence and abundance of mature microRNAs in the mouse brain. *Nucleic Acids Res.* **42**, 12155–12168
21. Heale, B. S. E., Keegan, L. P., McGurk, L., Michlewski, G., Brindle, J., Stanton, C. M., Caceres, J. F., and O'Connell, M. A. (2009) Editing independent effects of ADARs on the miRNA/siRNA pathways. *EMBO J.* **28**, 3145–3156
22. Riedmann, E. M., Schopoff, S., Hartner, J. C., and Jantsch, M. F. (2008) Specificity of ADAR-mediated RNA editing in newly identified targets. *RNA* **14**, 1110–1118
23. George, C. X., and Samuel, C. E. (1999) Characterization of the 5'-flanking region of the human RNA-specific adenosine deaminase ADAR1 gene and identification of an interferon-inducible ADAR1 promoter. *Gene* **229**, 203–213
24. Eckmann, C. R., Neunteufl, A., Pfaffstetter, L., and Jantsch, M. F. (2001) The human but not the Xenopus RNA-editing enzyme ADAR1 has an Atypical nuclear localization signal and displays the characteristics of a shuttling protein. *Mol. Biol. Cell* **12**, 1911–1924
25. Tan, M. H., Li, Q., Shanmugam, R., Piskol, R., Kohler, J., Young, A. N., Liu, K. I., Zhang, R., Ramaswami, G., Ariyoshi, K., Gupte, A., Keegan, L. P., George, C. X., Ramu, A., Huang, N., *et al.* (2017) Dynamic landscape and regulation of RNA editing in mammals. *Nature* **550**, 249–254
26. Li, L., Song, Y., Shi, X., Liu, J., Xiong, S., Chen, W., Fu, Q., Huang, Z., Gu, N., and Zhang, R. (2018) The landscape of miRNA editing in animals and its impact on miRNA biogenesis and targeting. *Genome Res.* **28**, 132–143
27. Ekdahl, Y., Farahani, H. S., Behm, M., Lagergren, J., and Öhman, M. (2012) A-to-I editing of microRNAs in the mammalian brain increases during development. *Genome Res.* **22**, 1477–1487

28. Vesely, C., Tauber, S., Sedlazeck, F. J., von Haeseler, A., and Jantsch, M. F. (2012) Adenosine deaminases that act on RNA induce reproducible changes in abundance and sequence of embryonic miRNAs. *Genome Res.* **22**, 1468–1476
29. Behm, M., Wahlstedt, H., Widmark, A., Eriksson, M., and Öhman, M. (2017) Accumulation of nuclear ADAR2 regulates adenosine-to-inosine RNA editing during neuronal development. *J. Cell Sci.* **130**, 745–753
30. Liddicoat, B. J., Piskol, R., Chalk, A. M., Ramaswami, G., Higuchi, M., Hartner, J. C., Li, J. B., Seeburg, P. H., and Walkley, C. R. (2015) RNA editing by ADAR1 prevents MDA5 sensing of endogenous dsRNA as nonself. *Science* **349**, 1115–1120
31. Macbeth, M. R., Schubert, H. L., VanDemark, A. P., Lingam, A. T., Hill, C. P., and Bass, B. L. (2005) Inositol hexakisphosphate is bound in the ADAR2 core and required for RNA editing. *Science* **309**, 1534
32. Yang, W., Chendrimada, T. P., Wang, Q., Higuchi, M., Seeburg, P. H., Shiekhattar, R., and Nishikura, K. (2006) Modulation of microRNA processing and expression through RNA editing by ADAR deaminases. *Nat. Struct. Mol. Biol.* **13**, 13–21
33. Kawahara, Y., Zinshteyn, B., Chendrimada, T. P., Shiekhattar, R., and Nishikura, K. (2007) RNA editing of the microRNA-151 precursor blocks cleavage by the Dicer–TRBP complex. *EMBO Rep.* **8**, 763–769
34. Ota, H., Sakurai, M., Gupta, R., Valente, L., Wulff, B.-E., Ariyoshi, K., Iizasa, H., Davuluri, R. V., and Nishikura, K. (2013) ADAR1 forms a complex with Dicer to promote microRNA processing and RNA-induced gene silencing. *Cell* **153**, 575–589
35. Chen, Y., and Wang, X. (2020) miRDB: An online database for prediction of functional microRNA targets. *Nucleic Acids Res.* **48**, D127–D131
36. Marvin, J. S., Shimoda, Y., Magloire, V., Leite, M., Kawashima, T., Jensen, T. P., Kolb, I., Knott, E. L., Novak, O., Podgorski, K., Leidenheimer, N. J., Rusakov, D. A., Ahrens, M. B., Kullmann, D. M., and Looger, L. L. (2019) A genetically encoded fluorescent sensor for *in vivo* imaging of GABA. *Nat. Methods* **16**, 763–770
37. Eshaq, R. S., Stahl, L. D., Stone, R., Smith, S. S., Robinson, L. C., and Leidenheimer, N. J. (2010) GABA acts as a ligand chaperone in the early secretory pathway to promote cell surface expression of GABAA receptors. *Brain Res.* **1346**, 1–13
38. Wang, P., Eshaq, R. S., Meshul, C. K., Moore, C., Hood, R. L., and Leidenheimer, N. J. (2015) Neuronal gamma-aminobutyric acid (GABA) type A receptors undergo cognate ligand chaperoning in the endoplasmic reticulum by endogenous GABA. *Front. Cell. Neurosci.* **9**, 188
39. Wahlstedt, H., Daniel, C., Enstërö, M., and Ohman, M. (2009) Large-scale mRNA sequencing determines global regulation of RNA editing during brain development. *Genome Res.* **19**, 978–986
40. Lundin, E., Wu, C., Widmark, A., Behm, M., Hjerling-Leffler, J., Daniel, C., Öhman, M., and Nilsson, M. (2020) Spatiotemporal mapping of RNA editing in the developing mouse brain using *in situ* sequencing reveals regional and cell-type-specific regulation. *BMC Biol.* **18**, 6
41. Hwang, T., Park, C.-K., Leung, A. K. L., Gao, Y., Hyde, T. M., Kleinman, J. E., Rajpurohit, A., Tao, R., Shin, J. H., and Weinberger, D. R. (2016) Dynamic regulation of RNA editing in human brain development and disease. *Nat. Neurosci.* **19**, 1093–1099
42. Costa Cruz, P. H., Kato, Y., Nakahama, T., Shibuya, T., and Kawahara, Y. (2020) A comparative analysis of ADAR mutant mice reveals site-specific regulation of RNA editing. *RNA* **26**, 454–469
43. Khvorova, A., Reynolds, A., and Jayasena, S. D. (2003) Functional siRNAs and miRNAs exhibit strand bias. *Cell* **115**, 209–216
44. Schwarz, D. S., Hutvágner, G., Du, T., Xu, Z., Aronin, N., and Zamore, P. D. (2003) Asymmetry in the assembly of the RNAi enzyme complex. *Cell* **115**, 199–208
45. Matranga, C., Tomari, Y., Shin, C., Bartel, D. P., and Zamore, P. D. (2005) Passenger-strand cleavage facilitates assembly of siRNA into Ago2-containing RNAi enzyme complexes. *Cell* **123**, 607–620
46. Rand, T. A., Petersen, S., Du, F., and Wang, X. (2005) Argonaute2 cleaves the anti-guide strand of siRNA during RISC activation. *Cell* **123**, 621–629
47. van der Kwast, R. V. C. T., Parma, L., van der Bent, M. L., van Ingen, E., Baganha, F., Peters, H. A. B., Goossens, E. A. C., Simons, K. H., Palmen, M., de Vries, M. R., Quax, P. H. A., and Nossent, A. Y. (2020) Adenosine-to-inosine editing of vasoactive microRNAs alters their targetome and function in ischemia. *Mol. Ther. Nucleic Acids* **21**, 932–953
48. Kozomara, A., Birgaoanu, M., and Griffiths-Jones, S. (2019) miRBase: From microRNA sequences to function. *Nucleic Acids Res.* **47**, D155–D162
49. Picardi, E., and Pesole, G. (2013) REDItools: high-throughput RNA editing detection made easy. *Bioinformatics* **29**, 1813–1814
50. Langmead, B. (2009) Ultrafast and memory-efficient alignment of short DNA sequences to the human genome. *Genome Biol* **10**, R25
51. Shannon, P., Markiel, A., Ozier, O., Baliga, N. S., Wang, J. T., Ramage, D., Amin, N., Schwikowski, B., and Ideker, T. (2003) Cytoscape: A software environment for integrated models of biomolecular interaction networks. *Genome Res.* **13**, 2498–2504
52. Bindea, G., Mlecnik, B., Hackl, H., Charoentong, P., Tosolini, M., Kirilovsky, A., Fridman, W.-H., Pagès, F., Trajanoski, Z., and Galon, J. (2009) ClueGO: A Cytoscape plug-in to decipher functionally grouped gene ontology and pathway annotation networks. *Bioinformatics* **25**, 1091–1093